24. THERMAL PROPERTIES OF TAG HYDROTHERMAL PRECIPITATES, MID-ATLANTIC RIDGE, AND COMPARISON WITH MIDDLE VALLEY, JUAN DE FUCA RIDGE[1]

Peter A. Rona,[2] Earl E. Davis,[3] and Rainer J. Ludwig[4]

ABSTRACT

To the few thermal conductivity measurements on sulfides/sulfates reported in the literature, we add 35 new values determined by two different methods for samples cored by Ocean Drilling Program (ODP) Leg 158 from the volcanic-hosted active sulfide mound in the TAG hydrothermal field, located in the rift valley of the Mid-Atlantic Ridge near 26°N, 45°W. Thermal conductivity measurements are essential to calculate heat flow and to model sulfide-hosted hydrothermal flow. Fifteen measurements were made on the ship by the half-space method, using a needle probe on seawater-saturated half-rounds of cores of heterogeneous mixtures of sulfide (predominantly pyrite), quartz, and anhydrite breccias. Values range between 6.1 and 10.4 W/(m·K); one measurement on anhydrite produced a value of 5.4 W/(m·K). At the Pacific Geoscience Centre, the divided bar method was used to measure twenty values on minicores extracted from other half-rounds of cores with similar mixed compositions and saturated with distilled water. These values range between 5.0 and 14.9 W/(m·K).

Despite scatter in the data, thermal conductivity values measured by the half-space method are systematically lower than those measured by the divided bar method. Measurements of sediment-hosted sulfides cored by ODP Leg 139 at the Bent Hill site, located at Middle Valley of the Endeavor segment of the northern Juan de Fuca Ridge, exhibited a similar discrepancy of values. Davis and Seeman (1994) and Gröschel-Becker et al. (1994) consider values produced by the half-space method to be systematically low for material with high conductivity because of a lack of calibration standards and the presence of nonlinear system behavior at high thermal conductivities. The TAG sulfides generally exhibit higher conductivities and lower porosities than the Middle Valley sulfides; this is attributable to higher pyrite content and more pore-filling quartz and/or anhydrite in the TAG location. Values of thermal conductivity measured in sulfides at both TAG and Middle Valley are high compared with values of seafloor sediment and basalt, which typically range between 1 and 2 W/(m·K). This marked contrast indicates that seafloor sulfide bodies may act as foci of conductive heat flow in addition to the spectacular convective thermal transfer by black smoker and diffuse venting.

INTRODUCTION

Ocean ridges are subject to intensive study as loci of transfer of heat and mass from the mantle to the crust and ocean by magmatic and related hydrothermal processes (RIDGE, 1992; Ocean Drilling Program [ODP], 1996). Conduction through crustal materials was initially considered to be the principal mode of heat transfer in ocean basins (Lee and Uyeda, 1965). Recognition of a large discrepancy between the calculated amount of heat supplied by the emplacement of lithosphere at ocean ridges and the measured conductive heat flow (Wolery and Sleep, 1976; Sclater et al., 1976) indicates the large-scale importance of convective hydrothermal circulation and associated advective heat transfer through the oceanic crust.

As a significant component of this transfer, vertical conductive heat flow is the product of thermal gradient and thermal conductivity of ocean crustal materials. The range of thermal conductivity in the widespread sediments and volcanic rocks of the seafloor is generally small (~0.8−2.5 W/[m·K]). However, little is known about thermal conductivity in the various types of hydrothermal precipitates (sulfides, sulfates, oxides, hydroxides; Clark, 1966; Kappelmeyer and Haenel, 1974; Roy et al, 1989) and associated alteration zones that exist at many sites along the global ocean ridge system (Rona and Scott, 1993). Drilling of the active sulfide mound in the TAG hydro-

thermal field, located in the rift valley of the Mid-Atlantic Ridge near 26°N, 45°W (Rona et al., 1993; Humphris et al., 1995), has yielded the first cores for measuring thermal conductivity in a volcanic-hosted, seafloor hydrothermal deposit. In this paper we present and evaluate values of thermal conductivity measured in TAG cores by two different methods, and we compare these findings with similar measurements made in hydrothermal precipitates recovered from a sediment-hosted hydrothermal deposit in the Middle Valley of the northern Juan de Fuca Ridge during Leg 139 (Mottl, Davis, Fisher, and Slack, 1994; Gröschel-Becker et al., 1994).

METHODS

Thermal Conductivity

The methods employed pertain to measurements of thermal conductivity and related properties of selected representative samples of sulfides, sulfates, silicates, and mixtures thereof cored from the TAG active sulfide mound during Leg 158 drilling. Thermal conductivity was measured on the ship by the half-space needle probe method and postcruise by the divided bar method. Thermal conductivity *(k)* of a substance is defined as the rate at which heat can be transferred by molecular conduction through it, such that *k* is the coefficient that gives the rate of heat transfer *(Q)* across a given steady-state temperature difference *(DT)* over a given distance *(Dx)* in a material in a one-dimensional sense (Fisher and Bontempo, 1991):

$$Q = k \, (DT / Dx).$$

Units of thermal conductivity are W/(m·K) for the amount of heat per second, where watts (W) is what is needed to make a material

[2]Peter A. Rona, Institute of Marine and Coastal Sciences and Department of Geological Sciences, Rutgers University, 71 Dudley Road, New Brunswick, NJ 08901-0521, U.S.A. rona@ahab.rutgers.edu

[3]Earl E. Davis, Geological Survey of Canada, Pacific Geoscience Centre, P.O. Box 6000, Sidney, British Columbia V8L 4B2, Canada.

[4]Rainer J. Ludwig, SOEST, University of Hawaii at Manoa, 2525 Correa Road, Honolulu, Hawaii 96822, U.S.A.

some distance (in meters [m]) from the heat source increase in temperature by some amount (in Kelvin [K] or °C).

Shipboard Half-Space Needle Probe Method

Shipboard measurements of thermal conductivity were made on 15 representative samples using the half-space needle probe method (Table 1). This method approximates the heating of a line source in a plane separating half spaces of the sample material and a thermal insulator, as an extension of the method of heating a uniform full space by a line source (Jaeger, 1956; Von Herzen and Maxwell, 1959). Although the half-space needle probe method assumes the application of the same theory as the full-space method, it requires a correction factor to account for the geometry of the experiment because the medium is assumed to be semi-infinite (Sass et al., 1984; Vacquier, 1985) rather than fully infinite.

The smoothly cut flat face of the archive half-round cylinder of a longitudinally split hard-rock core was submerged in a seawater bath and placed in contact with a needle probe mounted on an epoxy block. A thermal compound was applied to ensure good thermal contact between the flat face of the core and the needle probe; the thermal compound has a thermal conductivity of about 5–6 W/(m·K), which ensures that heat is not lost by advection (A.T. Fisher, pers. comm., 1996). This procedure is an adaptation of the full-space method, whereby the probe is inserted into the sediment, as described in the "Explanatory Notes" chapter of Alt, Kinoshita, Stokking, et al. (1993).

Thermal conductivity was calculated from the rate of temperature rise in the probe while a heater current was flowing, thereby employing a microcomputer-based unit under control of a host computer (Thermcon-85 box; Fisher and Bontempo, 1991). The temperature rise in the probe should vary logarithmically with time as

$$T(t) = (q / 4pk) \, ln(t) + \text{constant},$$

in which k is thermal conductivity, T and t are the temperature and time, respectively, and q is the heat generated per unit length of the probe. From this equation, thermal conductivity can be derived from the slope of temperature vs. the logarithm of time. A 60- to 240-s time interval was generally chosen to record these data following

practice on similar samples during ODP Leg 139 (see "Explanatory Notes" chapter of Davis, Mottl, Fisher, et al., 1991). If the substrate on which the sample is placed is a perfect thermal insulator, the rate of rise in temperature with time at the needle probe would be exactly twice that recorded by the probe in an infinite medium having the same thermal conductivity as the sample. In practice, the poorly conducting substrate (apparent thermal conductivities of the epoxy blocks are 0.2–0.3 W/[m·K]; Fisher and Bontempo, 1991) absorbs a fraction of the heat during the measurement, the amount of which depends primarily on the ratio of sample to substrate conductivity. For most rock samples measured during Leg 158, this ratio was sufficiently large so that the correction was relatively small.

The thermal conductivity probes were calibrated by measurements on three standards of known thermal conductivities (red rubber: 0.96 W/[m·K]; macor ceramic: 1.61 W/[m·K], and basalt: 2.05 W/[m·K]). All sample measurements were carefully monitored to achieve reproducible thermal conductivity values. After a good sample-probe contact was established, at least three measurements having very little post-measurement drift over time and giving similar values were completed. The thermal conductivity of the sample was taken as the average of the values obtained.

Postcruise Divided Bar Method

Thermal conductivities of 19 representative samples were measured on a divided bar apparatus postcruise at the Pacific Geoscience Centre (Table 2). The technique was first described by Lees (1892). The apparatus used for these measurements is similar to the one described by Beck (1957, 1988) and used by Davis and Seeman (1994) and Gröschel-Becker et al. (1994) to measure thermal conductivity in sediments, basalts, and sulfides cored during Leg 139. It consists of two constant-temperature baths at the top and bottom of a composite cylindrical "bar" forming the sample, bracketed symmetrically by a pair of copper measurement disks, a pair of standard disks, and a second pair of copper measurement disks. The baths maintained a 10°C temperature difference that was adjusted to evenly span the typical ambient laboratory temperature of 20°C. The exterior surface of the composite bar was insulated to reduce the radial heat loss and to ensure constant heat flow along the axis of the bar. After an equilibration period of 15–20 min, the thermal resistance of the sample was determined simply by comparing the temperature drop across the

Table 1. Leg 158 thermal conductivity measurements by shipboard needle probe method and related properties.

Hole, core, section	Half-round interval (cm)	Depth (mbsf)	Porosity (%)	Bulk density (kg/m^3)	Grain density (kg/m^3)	Electrical resistivity (Ωm)	Thermal conductivity (W/[m·K])	Lithology
158-957C-								
7N-1*	58-68	20.08	7.3	3740	3950	—	6.08	Nodular siliceous pyrite-anhydrite breccia
7N-2	64-76	21.49	—	—	—	—	8.73	Nodular siliceous pyrite-anhydrite breccia
7N-3*	10-25	22.45	9.6	2790	2980	2.767	5.37	Anhydrite vein
11N-1*	19-30	30.89	5.5	3280	3410	—	8.30	Pyrite-silica breccia
11N-2	28-36	32.39	—	—	—	—	8.68	Pyrite-silica-anhydrite breccia
14N-1**	10-22	40.30	4.6	3666	3794	0.091	8.34	Pyrite-silica breccia
15N-1*	110-119	43.30	3.6	3580	3670	0.411	8.65	Silicified wallrock breccia
16N-1	14-22	46.34	—	—	—	—	5.73	Nodular pyrite-silica breccia
16N-2	24-32	47.86	—	—	—	—	8.40	Silicified wallrock breccia
158-957F-								
1N-1**	52-64	1.52	11.9	3603	3953	0.518	6.10	Massive pyrite breccia
158-957G-								
3N-1**	6-20	21.06	12.4	4085	4519	0.114	8.59	Massive pyrite-anhydrite breccia
158-957H-								
5N-1**	29-40	26.99	9.2	3820	4110	0.584	†10.16/10.41	Nodular pyrite-silica breccia
5N-2*	27-33	27.87	9.9	4330	4690	0.068	†8.01/8.58	Silicified wallrock breccia
158-957O-								
2R-1**	30-40	8.24	10.2	4271	4639	0.078	10.48	Nodular pyrite breccia
4R-1*	23-34	16.19	7.8	4190	4460	0.191	10.15	Nodular pyrite-anhydrite breccia

Notes: — = no value. * = shipboard physical properties measurements in minicores within corresponding half-round of core; ** = postcruise physical properties measurements on minicores within corresponding half-round of core (Table 2). † = repeat measurements.

composite bar with that across the upper and lower standard disks. Comparison of the temperature drops across the two standards provided verification that radial heat loss was not a significant source of error. Calibration of the bar with an accurately known standard disk provided an estimate of the contact resistance of the composite bar stack, which was corrected for in the sample measurements.

The samples were 25.4-mm-diameter minicores cut for shipboard physical properties measurements. Final lengths of cores were measured after final preparation to within 0.1 mm and ranged from 22 to 25 mm. The minicores were cut from split rotary core barrel or motor-driven core barrel cores, with their axes perpendicular to the axis of the main core. Faces were trimmed with a diamond saw to be parallel. Any nonparallelism of the faces (typically well less than 1°) was accommodated by the gimbaled mount of the upper part of the divided bar apparatus. In a few cases, faces were lapped before measurement to improve surface flatness and smoothness. Surface roughness and chipped corners contribute to contact resistance that is not accounted for in the calibration of the bar. This can be a significant source of error and may cause measured conductivities to be systematically low. Most sample faces were smooth and intact. The faces of certain samples were poorer than average, with as much as 10%−20% of the face area damaged (Samples 158-957C-7-2, 28−30 cm; 158-957C-7N-3, 40−42 cm; 158-957C-16-1, 99−101 cm; 158-957M-9R-1, 75−77cm; 158-957F-1-1, 55−57 cm; and 158-957H-5N-2, 69−71 cm).

All samples had been oven-dried for shipboard porosity determinations and required resaturation for the conductivity measurements. Following the surface preparation, the samples were placed in a vacuum chamber evacuated to 0.15 atm for ~4 hr. They were immersed in distilled water while still under vacuum and then allowed to soak overnight at 1 atm. Samples were weighed before and after saturation; these values were combined with the sample volume estimated from the diameter and length to provide an estimate of porosity. These values agreed with the shipboard porosity determinations to within a few percent, confirming the completeness of saturation. To minimize evaporation during measurements, the minicores were wrapped in thin plastic sheeting before being insulated with a plastic foam jacket. As a final preparatory step, a viscous wetting agent (glycerine) was used on the minicore faces to reduce the errors caused by thermal contact resistance between the sample and copper measurement disks. A minimum of two, and up to four, repeat measurements were made on all samples. In some cases, samples were removed from the apparatus and resaturated before repeat measurements were made. Values were reproduced typically within 10%.

A suite of physical properties measurements for calculation of bulk density, grain density, porosity, and electrical resistivity were also made on all minicores that were extracted for the divided bar measurements. Half-round cylinders of cores were sampled at intervals considered representative of the various lithologies present (Shipboard Scientific Party, 1996). Whenever feasible, minicores were extracted from intervals opposite to the half-round cylinders on which the shipboard needle probe measurements of thermal conductivity were made (opposite 11 of 15 half-rounds; Tables 1, 2). Bulk density (kg/m³) is defined as the total wet sample mass divided by the total wet sample volume. Grain density (kg/m³) is defined as the mass of solids (mineral grains) divided by their volume. Porosity (%) is the ratio of the total volume of void spaces to the total wet sample volume.

RESULTS

Sensitivity to Mineralogy

Thermal conductivities measured by the shipboard half-space needle probe and the postcruise divided bar methods are presented in Tables 1 and 2. Values span a large range, roughly from 5 to 15 W/

(m·K), all very high compared with typical silicate rocks. This is evident in Figure 1, where conductivities of sulfide samples from the TAG active sulfide mound (this study) and the previously studied Mid Valley Bent Hill deposit (Leg 139, Site 856; Gröschel-Becker et al., 1994) are compared with conductivities of igneous and sedimentary rocks from the same areas (this study; Davis and Seeman, 1994). Values for sediments and igneous rocks typically fall between 1 and 2 W/(m·K) and are no higher than 3 W/(m·K).

Conductivities of the samples measured with the divided bar method are plotted with respect to sample porosity in Figure 1. Although the range of porosities of the TAG sulfide samples is relatively small, with most values falling between 5% and 15%, the range of thermal conductivities is large. This presumably reflects variations in the major mineral constituents and sample-to-sample differences in the way mineral grains contact one another. We examine these variations by considering two models that relate lithologic composition to bulk thermal conductivity. The geometric mean model (e.g., Drury and Jessup, 1983) is empirically based and widely used, especially for material of high porosity. The bulk conductivity, k_{Geo}, is defined as a function of the conductivities of the constituents of the aggregate, k_n, and the volumetric proportions of the constituents, ϕ_n:

$$k_{Geo} = \prod k_n{}^{\phi_n}.$$

Many physical models exist to account for bulk rock conductivity; several are discussed and compared by Beck (1988) and Roy et al., (1989). The one we have chosen describes a randomly dispersed mixture of mineral phases (Adler, 1973):

$$k_{Adl} = (\Sigma \phi_n (k_n)^{1/2})^2,$$

where k_{Adl} is the Adler mean thermal conductivity.

Other physical mixing models yield similar results at low porosities. Curves calculated for two-component theoretical mixtures, where $k_w = 0.6$ W/(m·K) and is the thermal conductivity of seawater, and k_{gr} is the effective average thermal conductivity of the constituent mineral grains, are shown for the three values of grain conductivity in Figure 1, using both the geometric and Adler mixing relationships. The lowest, $k_{gr} = 2.6$ W/(m·K), provides a good general fit to mafic igneous rocks and to the sediments sampled in Middle Valley during Leg 139, which contain mostly feldspar and clay minerals and small amounts of highly conductive quartz and carbonate minerals. Given the relatively small contrast between this grain conductivity and the conductivity of seawater, the curves defined by the two mixing relationships are nearly indistinguishable. The theoretical curves given for mixtures of water + pyrite, a mineral at the high end of the conductivity range (k_{gr} ~19.2 W/[m·K]; Clark, 1966), and water + anhydrite (k_{gr} ~5.4 W/[m·K]) bracket all of the sulfide data including those from the Bent Hill samples, which generally have higher porosities. Values falling near the lower limit of a composition field (Samples 158-957C-7N-2, 28−30 cm, and 158-957F-1N-1, 55−57 cm) may be erroneously low because of the poor quality of those sample faces, as described under the "Methods" section (this chapter).

The sulfides are actually heterogeneous mixtures in varying proportions of sulfide, anhydrite, quartz, and water. These four mineral phases were visually estimated by M.K. Tivey (Chapter 16, this volume) in thin sections of three specimens (Table 2; Sample 158-957C-7N-3, 47−49 cm: 80% pyrite + 20% chalcopyrite = 40% sulfide, 2%−5% quartz, 55%−58% anhydrite, 16% pore space, Adler mean 7.72 W/[m·K]; Sample 158-957C-11N-2, 22−24 cm: 75% pyrite + 25% chalcopyrite = 60% sulfide, 19% quartz, 18% anhydrite, 4.5% pore space, Adler mean 12.53 W/[m·K]; Sample 158-957C-14N-1, 18−20 cm: 98% pyrite + 2% chalcopyrite = 29% sulfide, 46% quartz, 22% anhydrite, 3.6% pore space, Adler mean 9.50 W/[m·K]). The Adler means (k_{Adl}) calculated for these three specimens exhibit a consistent

Table 2. Leg 158 thermal conductivity measurements by divided bar method and related properties.

Hole, core, section	Minicore interval (cm)	Depth (mbsf)	Porosity (%)	Bulk density (kg/m³)	Grain density (kg/m³)	Electrical resistivity (Ωm)	Thermal conductivity (W/[m·K])	Lithology
158-957C-								
7N-2	28-30	21.13	9.1	3415	3655	0.614	5.77 (?)	Nodular siliceous pyrite-anhydrite breccia
7N-3	40-42	22.75	15.4	3731	4222	0.383	7.83	Nodular pyrite-anhydrite breccia
7N-3*	47-49	22.81	15.9	3590	4100	0.265	10.24	Nodular pyrite-anhydrite breccia; *40% sulfide, 2-5% quartz, 55-58% anhydrite
11N-2†	18-20	32.29	5.5	4023	4198	0.107	13.58	Pyrite-silica-anhydrite breccia
11N-2*†	22-24	32.32	4.6	4150	4300	0.177	14.95	Pyrite-silica-anhydrite breccia; *60% sulfide, 19% quartz, 18% anhydrite
11N-2†	40-42	32.51	7.9	3677	3906	0.454	8.77	Veined pyrite-silica-anhydrite breccia
11N-3	112-114	34.73	6.6	3460	3633	0.636	12.21	Pyrite-silica breccia
13N-2	32-34	38.90	6.9	3766	3968	0.229	11.98	Pyrite-silica breccia with anhydrite veins
14N-1*	13-15	40.33	4.6	3666	3794	0.091	13.00	Pyrite-silica breccia
14N-1* †	18-20	40.37	3.5	3720	3820	0.502	13.85	Pyrite-silica breccia; *29% sulfide, 46% quartz, 22% anhydrite
15N-1	75-77	42.95	5.3	3651	3798	0.850	9.49	Silicified wallrock breccia
16N-1†	08-10	46.28	2.4	3373	3431	2.064	10.80	Nodular pyrite-silica breccia
16N-1	99-101	47.19	5.5	3692	3848	0.647	9.09	Silicified wallrock breccia
158-957F-								
1N-1†	55-57	1.55	11.9	3603	3953	0.518	5.02 (?)	Massive pyrite breccia
158-957G-								
3N-1†	15-17	21.15	12.4	4085	4519	0.114	14.24	Massive pyrite-anhydrite breccia
158-957H-								
5N-1* †	33-35	27.03	8.9	3820	4110	0.584	14.00	Nodular pyrite-silica breccia
5N-2 †	69-71	28.29	5.7	4042	4224	0.181	9.81	Silicified wallrock breccia with pyrite and cavities
158-957O-								
2R-1†	37-39	8.27	10.8	4011	4371	0.078	14.62	Nodular pyrite breccia
158-957O-								
4R-1†	40-42	16.30	10.2	4271	4639	0.026	13.81	Pyrite-anhydrite breccia
158-957M-								
9R-1	75-77	43.05	1.3	2922	2947	4.768	1.68	Basalt

Notes: * = M.K. Tivey, Chapter 16, this volume. † = Divided bar measurement on minicore within 10 cm of shipboard half-space needle probe measurement on half-round of core.

pattern that is lower (15%–30%) than the values measured (Table 2: 10.24 W/[m·K], 14.95 W/[m·K], and 13.85 W/[m·K], respectively), and lie between the anhydrite + water and pyrite + water curves shown in Figure 1.

The generally higher conductivities and lower porosities of the TAG sulfides compared with the Middle Valley sulfides are probably a consequence of the composition of the samples. The Middle Valley sulfides contain far less pore-filling quartz and/or anhydrite than the TAG sulfides and, in general, have a lower abundance of highly conductive pyrite (Gröschel-Becker et al., 1994). Of the TAG samples, the one having the lowest thermal conductivity (5.02 W/[m·K]; Sample 158-957F-1N-1, 55–57 cm; Table 2) is fine grained (~1 mm), and, although massive, it is friable and poorly cemented, much like many of the Middle Valley sulfides. This sample is the only TAG sample measured by the divided bar method with a thermal conductivity lower than a corresponding sample measured by the half-space needle probe method (Table 1; Sample 158-957F-1N-1, 52–64 cm; 6.10 W/[m·K]). This sample also is one of the minicores with poor faces, as noted under the "Methods" section (this chapter); therefore, the value is suspect.

In contrast, samples having high conductivities are highly competent. Although the sulfides in these samples are primarily brecciated, many sulfide breccia clasts of the high-conductivity samples are in direct contact with one another; elsewhere, excellent contact between clasts is provided by hydrothermal quartz cement. In some cases, the clasts are centimeter-scale. In two instances, the full lengths of the minicores are spanned by single massive clasts (e.g., Sample 158-957C-11N-2, 18–20 cm, 22–24 cm). Predictably, intermediate-conductivity samples are characterized by intermediate grain size (several millimeters) and clasts that are fully separated by quartz or anhydrite fill. This observation of the relationship between grain interconnectivity and thermal conductivity is supported by the determination of the degree of connectivity of pyrite grains in a quartz-anhydrite matrix, based on two-dimensional X-ray-computed tomography slices and petrographic thin sections of four of the samples by M.K. Tivey (Chapter 16, this volume; Table 2; Samples 158-957C-7N-3, 47–49 cm; 158-957C-11N-2, 22–24 cm; 158-957C-14N-1, 18–20 cm; 158-957H-5N-1, 33–35 cm).

A simple test of the influence of mineralogy on sample conductivity is provided in Figure 2, where estimated grain conductivity is plotted against the volumetric fill fraction assumed to consist of quartz (k = 7.7 W/[m·K]; ρ = 2650 kg/m^3) and anhydrite (k = 5.4 W/[m·K]; ρ = 2900 kg/m^3) in equal proportions. The fill fraction has been calculated from shipboard determinations of grain density (ρ) under the assumption that the solid fraction of the samples comprises a simple mixture of pyrite (k = 19.2 W/[m·K]; ρ = 4920 kg/m^3) and fill. Grain conductivities are calculated using an Adler mixing relationship and measured values of porosity and conductivity (Table 2). The line for a mixture of pyrite and fill shows an inverse relationship between grain conductivity and fill fraction and reflects the general trend of the data well.

DISCUSSION

Comparison of Half-Space Needle Probe and Divided Bar Measurements

Divided bar measurements made on the minicores are compared with shipboard measurements made on nearby half-round core cylinders (Fig. 3). Also included in the comparison are data obtained from samples of sediment, basalt, and sulfide collected during Leg 139 (Davis and Seeman, 1994; Gröschel-Becker et al., 1994). Data are somewhat scattered, probably partially because of the nonsystematic
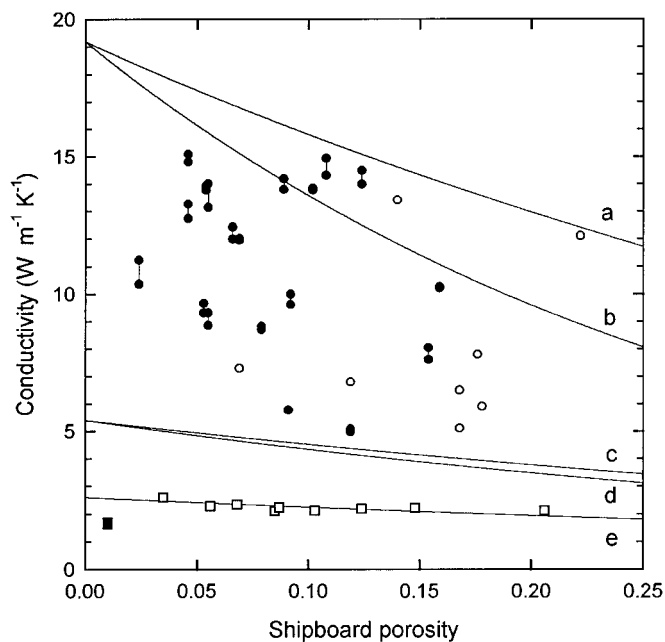

Figure 1. Thermal conductivity values measured with a divided bar plotted against porosity. Data from igneous and sedimentary rocks are shown as squares; data from sulfides are shown as circles. Solid circles are from the TAG deposit sampled during Leg 158; open circles are from Middle Valley sampled during Leg 139. Connected double circles show the range of repeat measurements. Curves are calculated for mixtures of pyrite + water (a and b), anhydrite + water (c and d), and sediment grains + water (e), using the commonly used Adler mean (a, c, and e) and geometric mean (b, d, and e) mixing relationships (see "Sensitivity to Mineralogy" section [this chapter] and the discussion in Beck [1988]).
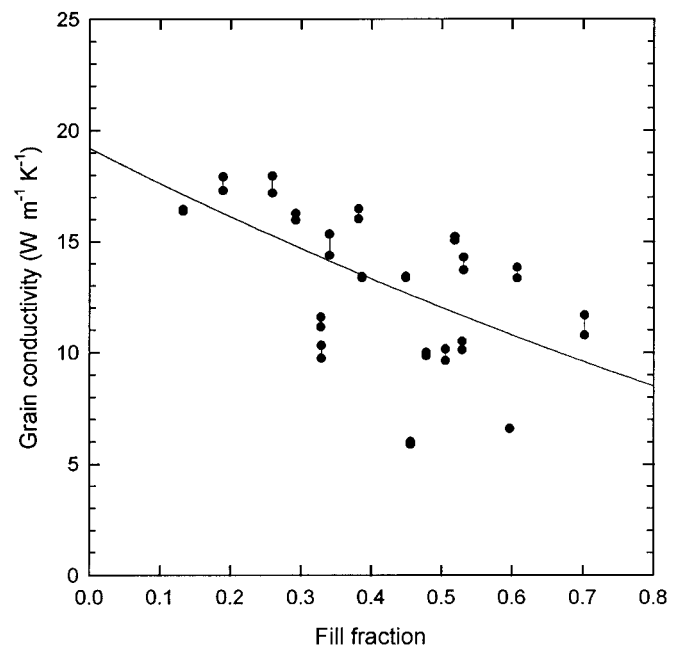

Figure 2. Estimated grain thermal conductivity vs. the estimated volumetric solid fraction of quartz + anhydrite fill within the sulfide-breccia samples. Fill, calculated from shipboard grain density, is assumed to consist of quartz (k = 7.7 W/[m·K]); ρ = 2650 kg/m^3) and anhydrite (k = 5.4 W/[m·K]); ρ = 2900 kg/m^3) in equal proportions. Grain conductivities are calculated using an Adler mixing relationship (Beck, 1988). The line is given for a mixture of pyrite (k = 19.2 W/[m·K]); ρ = 4920 kg/m^3) and fill.
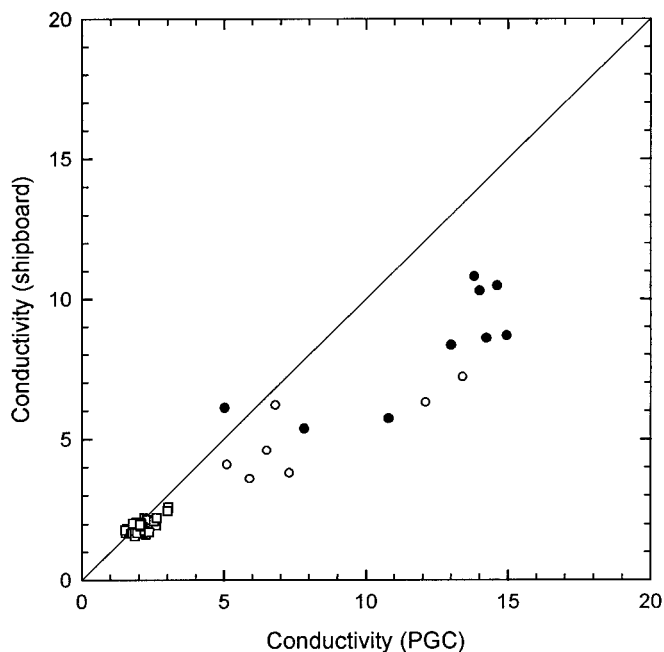
Figure 3. Thermal conductivity of core half-rounds based on shipboard measurement using the half-space needle probe method during Leg 158 vs. thermal conductivity of minicores collected typically within 10 cm of the half-round samples and measured at the Pacific Geoscience Centre using the divided bar method. Concordant measurements by the two methods would lie on the curve. Thermal conductivities are given in units of W/(m·K). Symbols for rock types and locations are the same as those shown in Figure 1.

errors inherent in the measurements, the combination of real local variations in the core, possible directional anisotropy related to sample orientation (half-rounds parallel to core axis; minicores perpendicular to core axis), and the noncoincidence of the measurement locations. However, despite the scatter, nearly all the sulfide data show a clear bias: shipboard measurements are systematically lower than the divided bar measurements. The bias was noted and the sources of the disagreement were discussed by Davis and Seeman (1994) and Gröschel-Becker et al. (1994). They concluded that the shipboard measurements are probably in error at high conductivities.

As presented in the "Methods" section (this chapter), shipboard measurements are made using the half-space technique in which a heated needle is imbedded in an epoxy block and is placed against the flat face of the split core. The data are first analyzed in a manner identical to a standard constant-heat-source needle probe method (Von Herzen and Maxwell, 1959), in which "absolute" values of conductivity are calculated from the slope of the temperature rise vs. the logarithmic time. Corrections for the nonaxisymmetric geometry are then adjusted with a linear correction factor, determined empirically by comparing the absolute measurements with known values of three calibration standards (Shipboard Scientific Party, 1992). The conductivities of these standards span the range normally encountered in sedimentary and igneous rocks (0.96–2.05 W/[m·K]). The range also spans values over which the postcruise divided bar and shipboard half-space measurements generally agree.

Unfortunately, the simple half-space correction appears to break down outside this range, probably for several reasons. One is that the characteristics of the system become nonlinear if the contrast between the conductivity of the sample and that of the material in which the line heat source is imbedded becomes large and, thus, the theory of cylindrical geometry cannot be applied. Another is that in the case

of high conductivity samples, the heat conducted from the line source will reach the sample boundaries within the measurement time and will then be limited by the relatively low conductivity of water. This will prevent extrapolation of calibration constants out to the very high values of these samples and will cause computed values of conductivity to be erroneously low. A correction could be applied to the half-space measurements using a best-fit line through the distribution of points shown in Figure 3. However, without a complete understanding of the bias and a proper check of the half-space apparatus with a high-conductivity calibration standard, such a correction is not advised.

CONCLUSIONS

Our study, comprising a shipboard investigation of thermal conductivity, using the needle probe method on 15 specimens representing diverse mixtures of high-temperature hydrothermal precipitates from the active sulfide mound in the TAG hydrothermal field, cored during Leg 158; postcruise measurement of thermal conductivity, using the divided bar method on 20 representative specimens from the TAG cores; and comparison of Leg 158 results with a similar study of high-temperature hydrothermal precipitates cored during Leg 139 at the Bent Hill site of Middle Valley, supports the following conclusions:

1. Shipboard thermal conductivity measurements by the half-space needle probe method are systematically too low in the conductivity range of high-temperature hydrothermal precipitates (5–15 W/[m·K]; i.e., low-porosity aggregates of sulfides, sulfates, and quartz). This phenomenon is attributed to multiple factors, including the breakdown of the theory for cylindrical geometry and sample boundary effects caused by high rates of heat conduction, and points to the need for calibration standards in that range.
2. Thermal conductivity in high-temperature hydrothermal precipitates is directly proportional to mechanical competence, average grain conductivity, and degree of interconnectivity of sulfide grains, which is consistent with the findings of M.K. Tivey (Chapter 16, this volume).

The contrast between thermal conductivity of widespread seafloor materials (sediments and basalt; 1–2 W/[m·K]) and localized massive sulfide bodies (5–15 W/[m·K]) is so large that the latter may act as foci of conductive heat transfer in addition to the high rates of convective heat transfer at seafloor hydrothermal fields.

ACKNOWLEDGMENTS

REFERENCES

Adler, D., Flora, L.P., and Sentura, S.D., 1973. Electrical conductivity in disordered systems. *Solid State Commun.,* 12:9−12.

Alt, J.C., Kinoshita, H., Stokking, L.B., et al., 1993. *Proc. ODP, Init. Repts.,* 148: College Station, TX (Ocean Drilling Program).

Beck, A.E., 1957. A steady state method for the rapid measurement of the thermal conductivity of rocks. *J. Sci. Instr.,* 34:185−189.

—————,1988. Methods for determining thermal conductivity and thermal diffusivity. *In* Haenel, R., Rybach, L., and Stegena, L. (Eds.) *Handbook of Terrestrial Heat-Flow Density Determination:* Dordrecht (Kluwer Academic Publishers), 87−124.

Clark, S.P., 1966. Thermal conductivity. *In* Clark, S.P. (Ed.), *Handbook of Physical Constants.* Mem.—Geol. Soc. Am., 97:461−482.

Davis, E.E., and Seeman, D.A., 1994. Anisotropic thermal conductivity of Pleistocene turbidite sediments of the northern Juan de Fuca Ridge. *In* Mottl, M.J., Davis, E.E., Fisher, A.T., and Slack, J.F. (Eds.), *Proc. ODP, Sci. Results,* 139: College Station, TX (Ocean Drilling Program), 559−564.

Drury, M.J., and Jessop, A.M., 1983. The estimation of rock thermal conductivity from mineral content: an assessment of techniques. *Zentralbl. Geol. Palaeontol.,* 1:35−48.

Fisher, A.T., and Bontempo, D.E., 1991. Thermal Conductivity and TC-PC Software Documentation: A User's Guide and Reference Manual (v140.1), Ocean Drilling Program.

Gröschel-Becker, H.M., Davis, E.E., and Franklin, J.M., 1994. Data Report: Physical properties of massive sulfide from Site 856, Middle Valley, northern Juan de Fuca Ridge. *In* Mottl, M.J., Davis, E.E., Fisher, A.T., and Slack, J.F. (Eds.), *Proc. ODP, Sci. Results,* 139: College Station, TX (Ocean Drilling Program), 721−724.

Humphris, S.E., Herzig, P.M., Miller, D.J., Alt, J.C., Becker, K., Brown, D., Brügmann, G., Chiba, H., Fouquet, Y., Gemmell, J.B., Guerin, G., Hannington, M.D., Holm, N.G., Honnorez, J.J., Itturino, G.J., Knott, R., Ludwig, R., Nakamura, K., Petersen, S., Reysenbach, A.-L., Rona, P.A., Smith, S., Sturz, A.A., Tivey, M.K., and Zhao, X., 1995. The internal structure of an active sea-floor massive sulphide deposit. *Nature,* 377:713−716.

Jaeger, J.C., 1956. Conduction of heat in an infinite region bounded internally by a circular cylinder of a perfect conductor. *Aust. J. Phys.,* 9:167−179.

Kappelmeyer, O., and Haenel, R., 1974. Geothermics. *Geoexpl. Monogr,. Ser. 1.*

Lee, W.H.K., and Uyeda, S., 1965. Review of heat flow data. *In* Lee, W.H.K. (Ed.), *Terrestrial Heat Flow.* Am. Geophys. Union, Geophys. Monogr., 8:87−186.

Lees, C.H., 1892. On the thermal conductivities of crystals and other bad conductors. *Philos. Trans. R. Soc. London A,* 183:491−509.

Mottl, M.J., Davis, E.E., Fisher, A.T., and Slack, J.F. (Eds.), 1994. *Proc. ODP, Sci. Results,* 139: College Station, TX (Ocean Drilling Program).

Ocean Drilling Program, 1996. Understanding Our Dynamic Earth through Ocean Drilling: Ocean Drilling Program Long Range Plan Into the 21st Century.

RIDGE, 1992. Science plan 1993−1997. *Ridge Interdiscipl. Global Exper.*

Rona, P.A., Hannington, M.D., Raman, C.V., Thompson, G., Tivey, M.K., Humphris, S.E., Lalou, C., and Petersen, S., 1993. Active and relict sea-floor hydrothermal mineralization at the TAG hydrothermal field, Mid-Atlantic Ridge. *Econ. Geol.,* 88:1987−2017.

Rona, P.A., and Scott, S.D., 1993. A special issue on sea-floor hydrothermal mineralization: new perspectives. *Econ. Geol.,* 88:1935−1975.

Roy, R.F., Beck, A.E., and Touloukian, Y.S., 1989. Thermophysical properties of rocks. *In* Touloukian, Y.S., Judd, W.R., and Roy, R.F. (Eds.), *Physical Properties of Rocks and Minerals* (Vol. I−2): New York (McGraw-Hill), 409−502.

Sass, J.H., Kennelly, J.P., Jr., Smith, E.P., and Wendt, W.E., 1984. Laboratory line-source methods for the measurement of thermal conductivity of rocks near room temperature. *U.S. Geol. Surv. Tech. Rep.,* 84−91.

Sclater, J.G., Crowe, J., and Anderson, R.N., 1976. On the reliability of ocean heat flow averages. *J. Geophys. Res.,* 81:2997−3006.

Shipboard Scientific Party, 1992. Explanatory notes. *In* Davis, E.E., Mottl, M.J., Fisher, A.T., et al., *Proc. ODP, Init. Repts.,* 139: College Station, TX (Ocean Drilling Program), 55−97.

—————, 1996. Explanatory notes. *In* Humphris, S.E., Herzig, P.M., Miller, D.J., et al., *Proc. ODP, Init. Repts.,* 158: College Station, TX (Ocean Drilling Program), 37−53.

Vacquier, V., 1985. The measurement of thermal conductivity of solids with a transient linear heat source on the plane surface of a poorly conducting body. *Earth Planet. Sci. Lett.,* 74:275−279.

Von Herzen, R.P., and Maxwell, A.E., 1959. The measurement of thermal conductivity of deep-sea sediments by a needle-probe method. *J. Geophys. Res.,* 64:1557−1563.

Wolery, T.J., and Sleep, N.H., 1976. Hydrothermal circulation and geochemical flux at mid-ocean ridges. *J. Geol.,* 84:249−275.